Brillouin-scattering study of the liquid-glass transition in supercooled aqueous lithium chloride solutions: Generalized hydrodynamics and mode-coupling analyses

N. J. Tao, G. Li, and H. Z. Cummins
Department of Physics, City College of The City University of New York, New York, New York 10031
(Received 13 July 1990)

Brillouin scattering in aqueous LiCl solutions was investigated in the concentration range 5–36 mol % at temperatures between 375 and 78 K. The polarized spectra were found to be accurately described by generalized hydrodynamics with a single-relaxation-time structural-relaxation process. The relaxation times obey the Arrhenius relation above ~200 K with activation energies between 2.5 kcal/mol at 36% and 6 kcal/mol at 5%. The transverse-acoustic mode that was observed in the depolarized spectra was qualitatively analyzed with a simple viscoelastic form for the transverse-current correlation function. The polarized spectra were also compared to preliminary predictions of the mode-coupling theory as formulated by Bengtzelius *et al.*, and showed qualitative agreement but significant quantitative disagreement. Both the LA and TA sound velocities exhibit discontinuous slope changes in their temperature dependences at the glass transition.

I. INTRODUCTION

The glass transition has been the subject of extensive experimental and theoretical studies for many years, both for its fundamental interest and for its practical importance.[1–6] Although it is widely believed that the glass transition is essentially kinetic, resulting from a "falling out of equilibrium" of density fluctuations in the liquid as the structural relaxation time increases with decreasing temperature, there is not yet a generally accepted complete theory of the transition. The free-volume model, combined with the ideas of percolation theory,[7] predicts that the glass transition is a first-order phase transition, while recent mode-coupling theories of the glass transition[8,9] imply that it is kinetic rather than thermodynamic. Experimentally, anomalies in thermodynamic properties such as the specific heat and thermal-expansion coefficients at a transition temperature T_g suggest a thermodynamic phase transition, while the observation that T_g depends on the cooling rate indicates that the transition is kinetic rather than thermodynamic. It is therefore still unclear whether or not the glassy state is distinct from the supercooled fluid in any sense beyond the infinite relaxation time.

Much of the dynamical information required for a full description of normal and supercooled fluids is contained in the density-correlation function $G(r,t)$ and its space-time Fourier transform, the dynamic structure factor $S(k,\omega)$. Polarized Raman-, Brillouin-, and quasielastic-light-scattering spectroscopy can determine $S(k,\omega)$ for frequencies from a few Hz out to the 10^{13}-Hz range characteristic of molecular vibrations. Brillouin scattering is especially useful for studying the glass transition since its range of $\sim 10^{-8}$–10^{-12} s includes the acoustic modes as well as the central-peak ("Mountain mode") scattering usually associated with structural relaxation processes. Molecular-dynamics simulations of liquid-glass transitions are also performed in this time regime[10,11] and therefore can be compared with Brillouin-scattering experiments.

Several Brillouin-scattering studies of liquids near the glass transition have been reported in the past, with analyses based on one of the generalized hydrodynamic approaches to be discussed in Sec. II. Materials previously studied include salol,[12,13] polymethyl acrylate,[14] and polymethyl methacrylate,[15] DMSO-H_2O,[16] (DMSO=dimethyl sulfoxide), triphenylphosphite,[17] B_2O_3,[18,19] $ZnCl_2$,[20,21] and [60% KNO_3–40% $Ca(NO_3)_2$].[19,22,23] In most cases, only the frequency shifts and linewidths of the Brillouin peaks were analyzed, while the additional information contained in the detailed spectral shape was ignored. Those studies in which the full spectrum was analyzed, such as the recent study of $ZnCl_2$ by Soltwisch *et al.*,[21] have shown that generalized hydrodynamics, which reduces to classical viscoelasticity in the long-wavelength limit appropriate for light-scattering experiments, can provide an excellent fit to the complete experimental data.

There is, however, an essential problem with the generalized hydrodynamics or viscoelasticity approach since an additional internal degree of freedom ξ with relaxation time τ which describes the structural relaxation process is introduced *ad hoc* and τ is adjusted to fit the data with no fundamental theoretical justification.

Mode-coupling theories, in contrast, require no *ad hoc* assumptions or extra degrees of freedom. Instead, the nonlinear coupling of a density fluctuation to two (or more) other density fluctuations is analyzed with no adjustable parameters, and a slow relaxation process emerges naturally from the theory. This approach has led to a renewal of interest in the glass transition, and several experiments have been analyzed to test some of

the specific predictions of the theory.[24–27] To date, however, there has been no analysis of Brillouin-scattering data based on the mode-coupling theory.

We have carried out a new Brillouin-scattering study of aqueous LiCl solutions which are good glass formers in the concentration range of 11–30 mol %. We studied solutions with concentrations of 5, 10, 12, 15, 30, and 36 mol % at temperatures from 375 to 78 K, and analyzed the data both with generalized hydrodynamics and with an approximate form of the mode-coupling theory.

We will review the approach of generalized hydrodynamics in Sec. II, and of the mode-coupling theory in Sec. III. Our experiments and the material studied are described in Sec. IV, and the polarized scattering results are analyzed in Sec. V. An analysis of the depolarized spectra is presented separately in Sec. VI, and discussion and conclusions are given in Sec. VII.

II. GENERALIZED HYDRODYNAMICS

In 1966, Mountain[28] analyzed the dynamic structure factor $S(k,\omega)$ [which is proportional to the polarized-light-scattering spectrum $I_{vv}(k,\omega)$] for a fluid with internal relaxation in the classical continuum limit of hydrodynamics. The kinetic bulk viscosity in the longitudinal part of the Navier-Stokes equation was generalized to include a frequency-dependent viscosity function $b'(\omega)$ which was then approximated by a single-relaxation-time expression

$$b'(\omega)=b_1/(1+i\omega\tau) .$$

(This approach is equivalent to the Maxwell theory of viscoelasticity.)

Mountain showed that

$$S(k,\omega)=S(k)2\,\mathrm{Re}\left[\frac{F(s)}{G(s)}\right]_{s=i\omega} , \tag{2.1}$$

where $F(s)$ and $G(s)$ are third- and fourth-order polynomials in s, respectively, and $S(k)$ is the static structure factor.

Equation (2.1) can be approximately separated into the sum of four terms: two Brillouin components centered near $\omega=\pm Ck$, where C is the adiabatic sound speed and k is the scattering vector, a quasielastic Rayleigh (thermal-diffusion) mode of width

$$\Gamma_T=D_Tk^2=\lambda k^2/\rho_0C_P ,$$

where λ is the thermal conductivity, ρ_0 is the average density, and C_P is the specific heat, and a fourth quasielastic mode (the Mountain mode) of width $\approx 1/\tau$, associated with the internal relaxation process. Although this factorization is qualitatively useful, the complete expression (2.1) should be used for the detailed analysis of spectra as emphasized by Mountain.[29] Further discussion of the general versus approximate form can be found in Montrose *et al.*[30]

The general result [Eq. (2.1)] can be simplified considerably for frequencies in the regime available to Brillouin spectroscopy for which ω is always much greater than $(\lambda/\rho_0C_P)k^2$, the width of the Rayleigh line. In this case, Eq. (2.1) becomes

$$S(k,\omega)=\frac{S(k)2(C_0^2k^2/\gamma)[b_0k^2+b_1k^2/(1+\omega^2\tau^2)]}{[\omega^2-C_0^2k^2-b_1k^2\omega^2\tau/(1+\omega^2\tau^2)]^2+[\omega b_0k^2+\omega b_1k^2/(1+\omega^2\tau^2)]^2} , \tag{2.2}$$

where $b_0=(\frac{4}{3}\eta_s+\eta_v)/\rho_0$ is the nonrelaxing (i.e., high-frequency) part of the longitudinal kinematic viscosity.

In a subsequent paper, Mountain[31] followed the alternative procedure of writing the hydrodynamic equations with frequency-independent transport coefficients, and introducing another coordinate ξ to represent the internal relaxing degree of freedom. Zwanzig[32] had previously shown that frequency-dependent transport coefficients in fluids result from internal degrees of freedom. Two cases were considered: in one, ξ couples to the local temperature (thermal relaxation); in the other, ξ couples to the local density (structural relaxation). The structural relaxation case was shown to reduce to the generalized bulk viscosity analysis resulting in Eq. (2.1), while the thermal relaxation case gave slightly different results. In LiCl solutions, the thermal relaxation process can be shown to be unimportant for Brillouin scattering, as discussed below.

The distinction between thermal relaxation and structural relaxation was further studied by Allain-Demoulin *et al.*[33] who analyzed the general mixed-coupling case and explored the interaction of the Rayleigh and Mountain modes near the transition, which is critically dependent on the type of coupling. [Although this aspect of the structure of $S(k,\omega)$ is crucial in analyzing the low-frequency spectrum observed in correlation spectroscopy, it is not important for Brillouin scattering where the Rayleigh line is not resolved.]

This mixed-coupling analysis was applied to the analysis of the light-scattering spectra of glycerol near its glass transition by Lallemand and his co-workers,[34] and recently to salol by Sidebottom and Sorenson.[35] Allain-Demoulin *et al.*[33] also extended the structural relaxation analysis to nonexponential relaxation by introducing N coordinates ξ_i, with relaxation times τ_i. An important result of their analysis was that, if the frequency-dependent bulk viscosity is represented by a phenomenological function such as the Cole-Davidson distribution, the parameters of the fit are very different from those found with a frequency-dependent longitudinal elastic modulus.

The Mountain approach described above is a viscoelas-

tic generalization of classical hydrodynamics to include slowly relaxing degrees of freedom that applies in the long-wavelength (small-k) limit in which the continuum approximation is valid. In the next section we will need to consider density fluctuation modes at much larger wave vectors for which the continuum hydrodynamic theory is inapplicable. The generalization of $S(k,\omega)$ to large-k values where the molecular structure of the liquid becomes important is a complex problem encompassed by the program of molecular hydrodynamics. A detailed treatment of this approach can be found in the book by Boon and Yip.[36]

A suitable generalization of $S(k,\omega)$ which covers the full range of interest of k and ω is [cf. Ref. 36, Eqs. (6.3.12) and (6.3.36)]

$$S(k,\omega)=\left[\frac{k}{\omega}\right]^2 v_0^2 \frac{\omega^2 k^2 D'(k,\omega)}{\{\omega^2-[(kv_0)^2/S(k)]+\omega k^2 D''(k,\omega)\}^2+[\omega k^2 D'(k,\omega)]^2} , \tag{2.3}$$

where v_0 is the thermal velocity $(k_B T/m)^{1/2}$,

$$D'(k,\omega)=\frac{(\gamma-1)v_0^2}{S(k)}\frac{D_T k^2}{\omega^2+(D_T k^2)^2}+\Phi_l'(k,\omega) , \tag{2.4}$$

$$D''(k,\omega)=\frac{-(\gamma-1)v_0^2}{S(k)}\frac{\omega}{\omega^2+(D_T k^2)^2}-\Phi_l''(k,\omega) . \tag{2.5}$$

$\Phi_l(k,\omega)$ is the Fourier transform of $\Phi_l(k,t)$, the memory function for the longitudinal kinematic viscosity $\nu_l=(\frac{4}{3}\eta_s+\eta_B)/\rho_0$, and $D_T k^2$ is the width of the thermal-diffusion (Rayleigh) mode.

Since the thermal-diffusion mode is much too narrow to resolve in a Brillouin-scattering experiment, the limit $\omega \gg D_T k^2$ applies, and

$$\omega k^2 D''(k,\omega)=\frac{-(\gamma-1)(kv_0)^2}{S(k)}+\omega k^2 \Phi_l''(k,\omega) , \tag{2.6}$$

while the first term in $D'(k,\omega)$ can be ignored. Therefore,

$$S(k,\omega)=\frac{(v_0 k^2)^2 \Phi_l'(k,\omega)}{\{\omega^2-[\gamma(kv_0)^2/S(k)]+\omega k^2 \Phi_l''(k,\omega)\}^2+[\omega k^2 \Phi_l'(k,\omega)]^2} . \tag{2.7}$$

In the hydrodynamic (long-wavelength) limit

$$\gamma(kv_0)^2/S(k)\rightarrow C_0^2 k^2 ,$$

where C_0 is the low-frequency adiabatic sound velocity, so that

$$S(k,\omega)=\frac{(v_0 k^2)^2 \Phi_l'(k,\omega)}{[\omega^2-C_0^2 k^2+\omega k^2 \Phi_l''(k,\omega)]^2+[\omega k^2 \Phi_l'(k,\omega)]^2} . \tag{2.8}$$

If we make the single-relaxation-time approximation for the relaxing part of the viscosity memory function

$$\Phi_l^R(k,t)=\Phi_l(k,0)e^{-t/\tau_l(k)}$$

and separately represent the nonrelaxing part of the longitudinal viscosity by Φ_0, then Eq. (2.8) becomes

$$S(k,\omega)=\frac{(v_0 k^2)^2\{\Phi_0+\Phi_l(k,0)\tau_l(k)/[1+\omega^2\tau_l^2(k)]\}}{\{\omega^2-C_0^2 k^2-\omega^2 k^2 \Phi_l(k,0)\tau_l^2(k)/[1+\omega^2\tau_l(k)^2]\}^2+\{\omega\Phi_0 k^2+\omega k^2 \Phi_l(k,0)\tau_l(k)/[1+\omega^2\tau_l^2(k)]\}^2} . \tag{2.9}$$

Equation (2.9) recovers the reduced form of the Mountain equation (2.2) if we replace $\tau_l(k)$ by τ, Φ_0 by b_0, and Φ_l by b_1/τ.

Note that, if temperature fluctuations represented by the first terms in D' and D'' in Eqs. (2.4) and (2.5) are neglected from the beginning, the resulting equations (2.7)–(2.9) would be unchanged except that C_0 would be the isothermal rather than the adiabatic sound speed and $\gamma=1$.

III. MODE-COUPLING THEORY

In 1984, Bengtzelius *et al.*[9] and Leutheusser[8] proposed a dynamical model of the liquid-glass transition, which was further developed by *inter alia* Gotze, Sjorgen, and Bengtzelius,[37–39] Kirkpatrick,[40] and Marchetti.[41] In this model, a dynamical density fluctuation with wave vector k can couple to two (or more) other density fluctuations with overall k conservation. This nonlinear coupling

causes a density-dependent renormalization of the dynamic structure factor leading to an increase of the transverse and longitudinal viscosities and eventual freezing of the fluctuations at a critical density associated with the glass transition.

Following Bengtzelius *et al.*[9] we begin with a complex dynamic structure factor

$$\tilde{S}(k,\omega)=\frac{k^2}{\omega^2}J(k,\omega) ,$$

the Fourier transform of the density correlation function $F(\mathbf{k},t)=\langle \delta n(\mathbf{k},0)\delta n(-\mathbf{k},t)\rangle$:

$$\tilde{S}(k,\omega)=\frac{(k^2/\omega^2)v_0^2}{\{-i\omega+(i/\omega)[(kv_0)^2/S(k)]+M(k,\omega)\}}+\frac{i}{\omega}S(k) . \tag{3.1a}$$

[Taking the real part of Eq. (3.1A) recovers the result of Eq. (2.7) with

$$M(k,\omega)=k^2\Phi_l(k,\omega)$$

and $\gamma=1$.] Equation (3.1a) can also be written as

$$\tilde{R}(k,\omega)=\frac{i}{\omega-(kv_0)^2/[S(k)(\omega+iM)]}=\frac{i}{\omega-\omega_0^2/(\omega+iM)} , \tag{3.1b}$$

where $\tilde{R}(k,\omega)=\tilde{S}(k,\omega)/S(k)$ is the normalized complex dynamic structure factor and $\omega_0^2=(kv_0)^2/S(k)$.

The generalized damping function $M(k,\omega)$ in Eq. (3.1) is next separated into two parts:

$$M(k,\omega)=\Gamma_0(k)+\Gamma_{\mathrm{MC}}(k,\omega) , \tag{3.2}$$

where Γ_0 is a background damping term proportional to k^2 representing all high-frequency (nonrelaxing) processes, and the mode-coupling part $\Gamma_{\mathrm{MC}}(k,\omega)$ includes the important structural dynamics.

The leading two-mode approximation for $\Gamma(k,t)$, the Fourier transform of $\Gamma_{\mathrm{MC}}(k,\omega)$, is

$$\Gamma(k,t)=(2\pi)^{-3}\int d^3\mathbf{k}'V(\mathbf{k},\mathbf{k}')R(\mathbf{k}',t)R(|\mathbf{k}-\mathbf{k}'|,t) , \tag{3.3}$$

where $R(k,t)$ is the Fourier transform of $R(k,\omega)$ and the vertex (or coupling) constant $V(k,k')$ is given by

$$V(\mathbf{k},\mathbf{k}')=(n/m\beta)(\hat{\mathbf{k}}\cdot\mathbf{k}')C(\mathbf{k}')\times\{(\hat{\mathbf{k}}\cdot\mathbf{k}')C(\mathbf{k}')+[\hat{\mathbf{k}}\cdot(\mathbf{k}-\mathbf{k}')]C(|\mathbf{k}-\mathbf{k}'|)\}\times S(\mathbf{k}')S(|\mathbf{k}-\mathbf{k}'|) , \tag{3.4}$$

where $C(k)=[S(k)-1]/[nS(k)]$ is the direct correlation function.

Equations (3.1b),(3.2), and (3.3) permit a self-consistent determination of $\tilde{S}(k,\omega)$ for all k with only the static structure factor $S(k)$ and the density n as inputs. Starting with all $\Gamma_{\mathrm{MC}}(k,\omega)=0$ in Eq. (3.2) so that initially $M(k\omega)=\Gamma_0(k)$, $\tilde{S}(k,\omega)$ in (3.1) for each k is Fourier transformed to find $R(k,t)$; $\Gamma(k,t)$ is then evaluated from (3.3), and $M(k,\omega)$ [Eq. (3.2)] is corrected. This process is repeated until the $\tilde{S}(k,\omega)$ no longer change on additional iteration, producing the self-consistent mode-coupling (SCMC) result.

Analysis has shown that the major contribution to $\Gamma_{\mathrm{MC}}(k,\omega)$ comes from coupling to pairs of modes near k_0, the wave vector of the first peak of the static structure factor $S(k)$.[9,40] As an approximation to the full SCMC result, we therefore compute $\tilde{S}(k_0,\omega)$ self-consistently including only modes with $|k|=k_0$,[9] and subsequently analyze $\tilde{S}(k,\omega)$ for a long-wavelength hydrodynamic mode coupling to pairs of k_0 modes.

The angular integration in Eq. (3.3) is first carried out leading to the form for $\Gamma(k,t)$ given by Eq. (2.19) of Ref. 9. $S(k)$ is then approximated by [Ref. 9, Eq. (4.1)]

$$S(k)=1+A\delta(k-k_0) , \tag{3.5}$$

where A is the area under the first peak of $S(k)$ above a baseline of 1. This reduces the full mode-coupling contribution to $S(k_0,\omega)$ to a coupling to pairs of modes with $|k|=k_0$. Equation (3.3) then reduces to

$$\Gamma(k_0,t)=4\lambda\omega_0^2(k_0)R^2(k_0t) , \tag{3.6}$$

where

$$\lambda=\frac{k_0A^2}{32\pi^2n}S(k_0) \tag{3.7}$$

and

$$\omega_0^2(k_0)=\frac{k_0^2}{M\beta S(k_0)} .$$

Next, we used the Percus-Yevick approximation for a hard-sphere gas[42] to obtain A, k_0, and $S(k)$ as functions of the packing fraction $\psi=\pi n\sigma^3/6$, where σ is the hard-sphere diameter and n is the number density. The value of A in Eq. (3.5) for each ψ was found by integrating the area under the first peak of $S(k)$. These values were then all rescaled (increased by 68%) so that the glass transition would occur at $\psi_c=0.516$ as found by Bengtzelius *et al.*[9] (ψ_c is $\sim$70% of the fcc tight-packing fraction $\psi_{\mathrm{TP}}=0.740$ or 81% of the random-close-packing fraction $\psi_{\mathrm{RCP}}=0.637$.) $S(k_0,\omega)$ was computed for values of ψ from 0.38 to 0.516 by iteration of Eqs. (3.1), (3.2), and (3.6) until convergence was achieved which required $\sim$20 iterations. An approximate correspondence between ψ and T was imposed by setting the glass transition ($\psi_c=0.516$) at $T_g=140$ K and then utilizing the measured thermal expansion coefficient $\alpha=3\times10^{-4}$ K^{-1} of LiCl solutions.[43] The results are shown in Table I.

Our results for $\mathrm{Re}[R(k_0,\omega)]$ versus ω are plotted in Fig. 1. Note that, at small ψ ($\psi\leq0.4$), there is a maximum in the spectrum representing a propagating acousticlike mode. As ψ increases, this feature becomes overdamped and is replaced by a narrow relaxing feature (the slow structural relaxation process) and a broad spectrum of fast-relaxation processes. (See also Fig. 5 of Ref. 9.) The width of the narrow component goes to zero at $\psi_c=0.516$ where the density fluctuations "freeze" pro-

TABLE I. Coefficients for mode-coupling calculations (Percus-Yevick hard-sphere gas: $\sigma_0=4.5$ Å, $T_g=140$ K, $\alpha=3\times10^{-4}$ K^{-1}) $k_e=2.5\times10^5$ cm^{-1}.

η	T (K)	λ (k_0)	$k_0\sigma$	$S(k_0)$	$S(k_e)$	A
0.383	1000	0.210	6.58	1.93	4.65×10^{-2}	1.96
0.491	300	0.745	6.98	3.09	1.71×10^{-2}	3.17
0.496	270	0.775	7.00	3.17	1.63×10^{-2}	3.23
0.499	250	0.804	7.00	3.22	1.58×10^{-2}	3.28
0.502	230	0.837	7.02	3.28	1.53×10^{-2}	3.32
0.505	210	0.869	7.02	3.34	1.48×10^{-2}	3.36
0.508	190	0.905	7.04	3.40	1.44×10^{-2}	3.40
0.511	170	0.942	7.04	3.46	1.39×10^{-2}	3.45
0.5150	150	0.9785	7.06	3.52	1.35×10^{-2}	3.49
0.515 98	140	0.9998	7.08	3.556	1.33×10^{-2}	3.515

ducing the nonergodic glassy state. In the liquid phase close to ψ_c, the fast- and slow-relaxation processes each have weight of $\frac{1}{2}$.

Next, we computed $S(k,\omega)$ for a hydrodynamic mode starting from the SCMC results already obtained for $S(k_0,\omega)$. The long-wavelength form for $\Gamma(k,t)$ given by Eq. (2.20) of Ref. 9, with the δ-function approximation for $S(k)$ of Eq. (3.5), results in

$$\Gamma(k,t)\approx\left[\frac{k}{k_0}\right]^2\frac{8\lambda k_0}{A}\omega_0^2(k_0)[S(k_0)-1]R^2(k_0,t)$$

$$\approx\frac{2}{k_0 A}[S(k_0)-1]k^2\Gamma(k_0,t)\ . \tag{3.8}$$

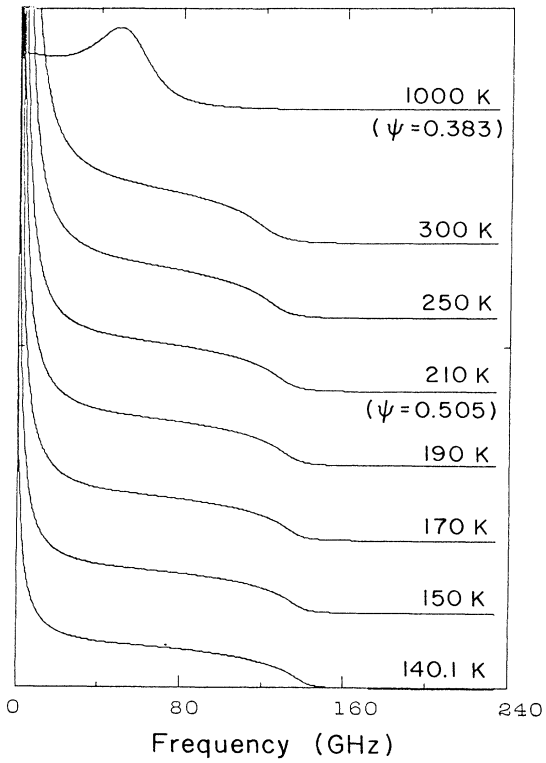

FIG. 1. Mode-coupling theory predictions for $S(k_0,\omega)$ at temperatures between 1000 and 140 K obtained from a self-consistent calculation involving modes with $|k|=k_0$ only as described in the text.

This expression for $\Gamma(k,t)$ was Fourier transformed, added to Γ_0 to give $M(k,\omega)$, and inserted in Eq. (3.1). We performed this calculation for $k_e\approx2.5\times10^5$ cm^{-1} ($k_e\sigma=0.0115$ with $\sigma=4.5$ Å) which is the appropriate value for our Brillouin-scattering experiments. The resulting spectra $\mathrm{Re}[R(k_e,\omega)]$ are plotted in Fig. 2 for the same values of ψ used in Fig. 1. However, the mode-coupling contribution of Eq. (3.8) has been multiplied by a factor of 7 to produce results close to those found in the experiment.

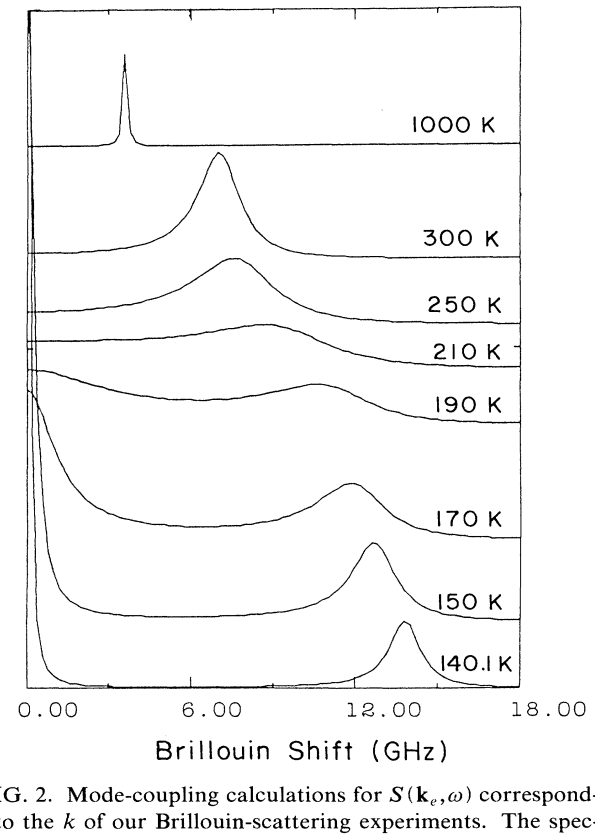

FIG. 2. Mode-coupling calculations for $S(\mathbf{k}_e,\omega)$ corresponding to the k of our Brillouin-scattering experiments. The spectra at $\eta=0.383$, corresponding to $T=1000$ K, indicates the residual linewidth due to Γ_0 when the mode-coupling contribution has essentially disappeared. Note that the coupling constant has been increased from its theoretical value by seven times.

IV. EXPERIMENTS

A. Materials

Aqueous LiCl solutions have been widely studied. In an extensive calorimetry study, Angell *et al.*[44,45] found that the glass-forming ability of this system is highly concentration dependent. Below 11 mol %, the nucleation of ice takes place as the sample is cooled; above 30%, crystallization also occurs easily and evidence shows that it corresponds to the formation of $LiCl \cdot n H_2O$ crystals.[46–48] However, at concentrations between these limits, it is a very good glass-forming system. Ionic aqueous solutions are also important for biological reasons; e.g., ions with water play critical roles in both the structure and dynamics of DNA.[49,50] There have been extensive structural and dynamical studies of LiCl.[51] Structural correlation functions have been measured by x-ray[52] and neutron-diffraction[53] experiments; dynamical properties, such as diffusion constants, ionic conductivity relaxation, and reorientational relaxations have been investigated by quasielastic neutron scattering,[54,55] dielectric measurements,[56] NMR,[57] and depolarized light scattering.[58] An early Brillouin-scattering study was reported by Hsich *et al.*[59]

B. Experimental procedures

In this paper, we report a study of Brillouin scattering in LiCl solutions at concentrations of 5, 10, 12, 15, 30, and 36 mol % from 375 to 78 K. The experiments were performed at scattering angles of 90° and 25° which correspond to a factor of 3 variation of scattering wave vector. Both polarized and depolarized spectra were investigated.

Sigma Reagent grade LiCl (99.5%) was used, and LiCl solutions were prepared using distilled deionized water. Each solution was filtered through a 0.2-μm membrane filter. The samples were clear; dust crossing the scattering column was rare. The solutions were loaded into cylindrical glass tubes with a diameter of 1 cm and sealed with a flame (the tube was kept in liquid nitrogen during the sealing so that evaporation was negligible). Each tube was fitted in a cylindrical copper block with four small windows for incident and scattered light, and the copper block was attached to the cold finger of an Oxford liquid-nitrogen cryostat. The temperature was controlled by an Oxford temperature controller with an accuracy of ~ 0.1 K. A platinum resistance thermometer was mounted close to the sample, which insured that the reading from the temperature controller was close to the temperature of the sample.

Spectra were collected using a Sandercock[60] six-pass tandem Fabry-Perot interferometer with a finesse >60. The advantage of the tandem interferometer over conventional Fabry-Perot interferometers has been discussed in several papers.[60,61] The high-resolution and high contrast enabled us to study the detailed shape of the whole polarized spectrum as well as the weak transverse modes in the depolarized spectrum. The single-mode 4880-Å line from a Spectra Physics model 165 argon-ion laser was used with a typical power of 50 mW. Light transmitted through the interferometer was detected by a Hamamatsu R464S photomultiplier tube and the digital data was recorded by an AT-type computer equipped with an EG&G multiscalar card.

In the experiments, the samples were cooled by steps of 5° or 10° with a cooling rate of about 1 K/min then kept constant for collecting a spectrum for 20 min. (For the weak transverse modes, the collecting time for a spectrum was about 2 h.) In this way, for the samples of 15 and 30 mol %, more than 30 spectra were obtained between 375 K and liquid-nitrogen temperature, and no crystallization occurred (i.e., no significant increase in the intensity of the elastically scattered light was observed). This result is consistent with Ref. 45. For 5, 10, and 36-mol %, samples, heterogeneous nucleation occurred during the cooling, which was unavoidable in our experiments even when a 10 K/min cooling rate was used. Nevertheless, some good spectra above the nucleation temperature were obtained with these samples. The 12-mol % solution, which lies at the boundary between good glass formers and good crystal formers, is of special interest. When the temperature was kept at a value below ~ 200 K, no immediate nucleation occurred, but after several minutes, the scattering column increased in brightness and finally became milky. A LiCi solution at a similar concentration was studied by neutron scattering,[46] which showed that crystallization corresponding to the formation of ice takes place at low temperatures. Spectra were also taken while heating the solution up to room temperature from liquid-nitrogen temperature; no observable difference was found between the cooling and heating runs.

In our experiments, 90° and near-forward (scattering angle equals 24°) scattering geometries were used. The collection angle was $\sim 4°$ for the 90° scattering and less than 2° for near-forward scattering. In both cases, the extra aperture broadening of the Brillouin linewidth is small and therefore was ignored in the data analysis. Both VV (vertically polarized scattered light collected with vertically polarized incident light) and VH (horizontally polarized scattered light collected with vertically polarized incident light) spectra were studied. The VV spectra always exhibited a longitudinal acoustic mode, while the VH spectra exhibited transverse acoustic modes only when T was low enough for $\omega\tau \gtrsim 1$ to be valid.

C. Results

1. Polarized (VV) spectra

The experimental Brillouin spectra of the 15-mol % LiCl solution at $\theta = 90°$ are shown by the circles in Fig. 3. At $T = 285$ K (the top spectrum in Fig. 3), the spectrum has the typical Rayleigh-Brillouin triplet form for a liquid, which consists of three peaks; the (unresolved) central Rayleigh component (it is too strong to show the entire peak on the scale of Fig. 3) and the two symmetrically shifted Brillouin peaks from the longitudinal sound waves. The Rayleigh component, which is attributed to combined entropy fluctuations and concentration fluctua-

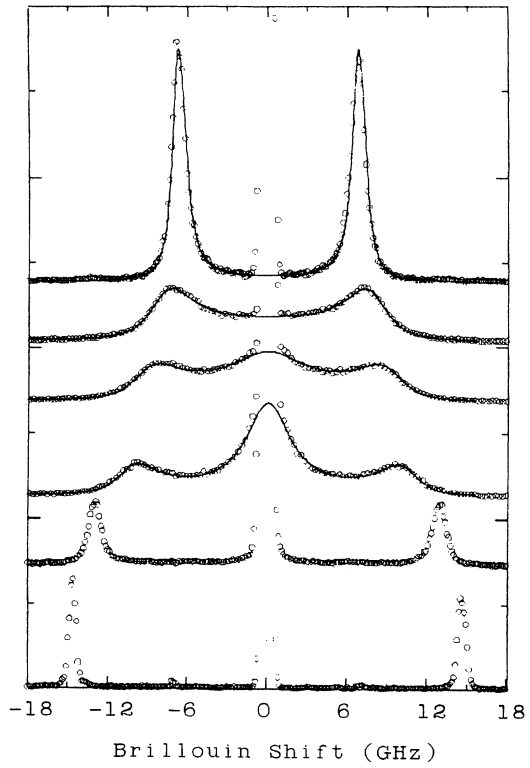

FIG. 3. VV Brillouin spectra of the 15-mol % LiCl solution at 285, 255, 245, 235, 200, and 180 K (from top to bottom). The circles are the experimental spectra, and the solid lines are the calculated spectra using Eqs. (2.9) or (5.1). (Only $\sim\frac{1}{4}$ of the data points are shown for clarity.)

tions in this experiment, has a much higher peak intensity than the Brillouin peaks, and a width which is smaller than the instrumental width. (A detailed study of the Rayleigh peak in LiCl solutions was reported by Hsich *et al.*[59]) As the sample is cooled (from top to bottom in Fig. 3), the frequency shift of the Brillouin peaks increases, while their linewidth increases and reaches a maximum at about 250 K, and then decreases. Associated with the changes of the Brillouin peaks, an additional central mode arises and narrows as the temperature decreases, and finally disappears into the wings of the Rayleigh peak.

Using the refractive index data of Ref. 59, we calculated the speed of longitudinal sound waves at various concentrations from the frequency shift of the Brillouin peaks and plotted the results in Fig. 4(a) as a function of temperature. The longitudinal sound speed of supercooled water taken from Ref. 62 is also shown as a dashed line in Fig. 4(a). While for all the concentrations the sound speed behaves in a qualitatively similar way, we note that the longitudinal sound speed at high temperature (which corresponds to C_0, the low-frequency sound speed) is rather unusual. It initially increases as the temperature decreases for concentrations higher than 15 mol %, which is normal in the sense that it is the same as most pure liquids, but it *decreases* for concentrations below 15 mol %, a unique property of liquid water, which is believed to be associated with its hydrogen-bonded tetrahedral structure.[63] This result indicates that, below 15 mol %, part of the water in the solution retains the structure of pure water. The attenuation of the LA mode at various concentrations extracted from the Brillouin linewidths is plotted in Fig. 4(b). The values near the maximum are only approximate because of the overlap of the Brillouin peaks with the central mode. We can see that the value of the attenuation increases as the LiCl concentration decreases, which is attributed to the temperature dependence of C_0 [the high-temperature speed of the LA mode shown in Fig. 4(a)].

The experiment was also performed in a near-forward-scattering geometry with $\theta=24.6°$. The evolution of the spectrum as a function of temperature is qualitatively similar to the $\theta=90°$ results. As shown in Fig. 5, the changes of sound speed [Fig. 5(a)] and attenuation [Fig. 5(b)] occur at lower temperature for the near-forward-scattering geometry. This can be easily understood in terms of the relaxation theory, as we will show in the next section.

2. *Depolarized (VH) spectra*

The depolarized Brillouin spectrum of LiCl aqueous solutions of various concentrations at temperatures above 273 K was studied in Ref. 58, where a weak Lorentzian central mode was observed and attributed to the reorientational relaxation of the water molecules in the solution. We extended the study down to liquid-nitrogen temperature. Figure 6 shows the VH spectrum of a 30-mol % solution at $\theta=90°$ as a function of temperature. From bottom to top, the temperature increases from 78 to 220 K. A well-defined transverse mode can be seen at low temperatures. With increasing temperature, the frequency and intensity of the transverse mode decrease, and the linewidth (damping) increases quite rapidly. In addition, a central mode appears and increases in width, and finally overwhelms the transverse mode at $T\cong 210$ K. This result is similar to the transverse mode in [60% KNO_3–40% $Ca(NO_3)_2$] (Refs. 19 and 22) and salol (Refs. 12 and 13) observed by Brillouin scattering. A remarkable result is that the transverse mode remains underdamped well above T_g. Since the mode is very weak, accurate measurements of linewidth and intensity are difficult in this system; but the transverse sound speed was extracted from the frequency shifts and the resulting shear modulus for the 15% and 30% solutions are plotted in Fig. 7. We can see that both sound speeds change sharply at T_g, which may indicate a common origin for the change of LA and TA modes at T_g.

The transverse sound speed in LiCl solutions between 14 and 17 mol % has also been measured by the ultrasonic technique,[64] and C_∞ was interpolated from the data at low temperature. Although the temperature-dependent result found in that experiment is generally the same as ours, the values determined at low temperatures are much lower than those found from our Brillouin data.

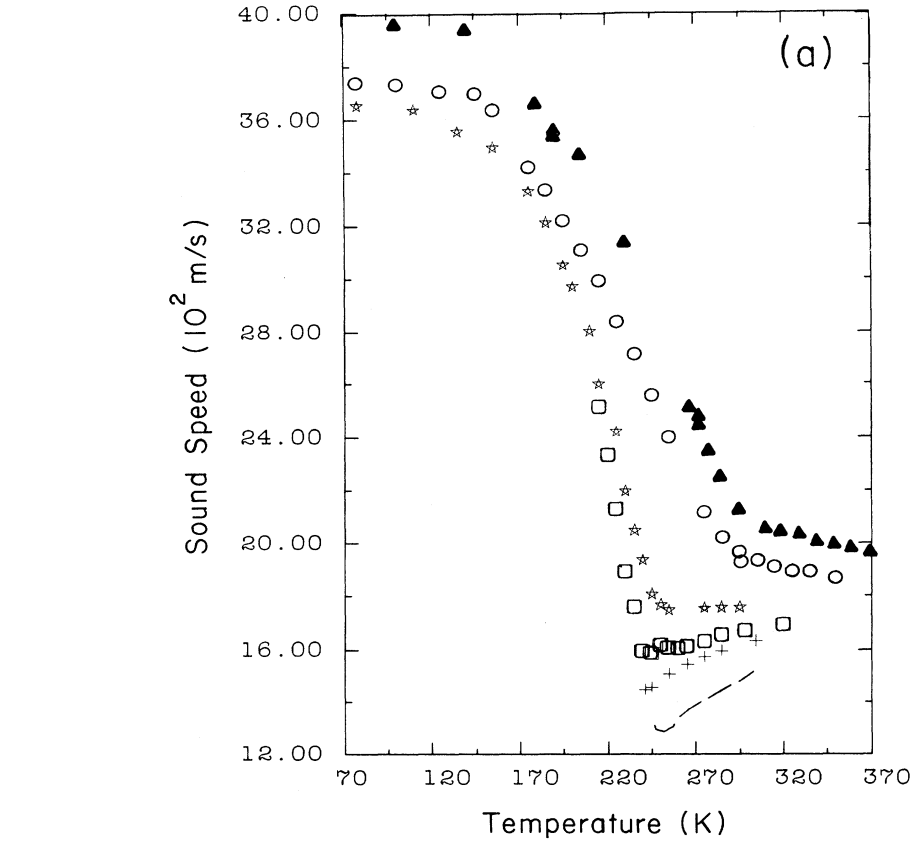

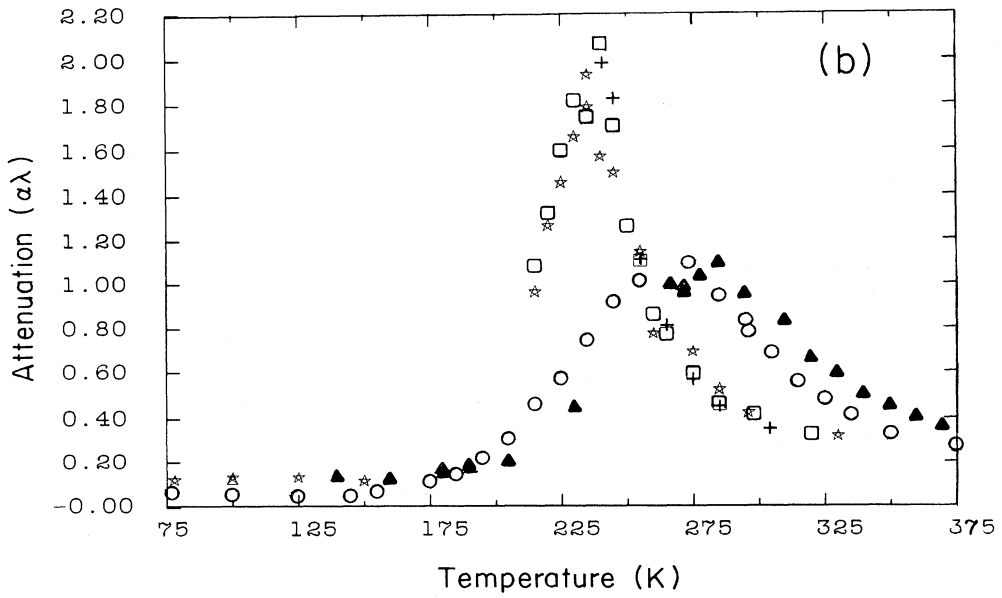

FIG. 4. The longitudinal sound speed (a) and the attenuation (b) found from Brillouin shifts and linewidths plotted against temperature. ▲, ○, ☆, □, and + represent the data of 36-, 30-, 15-, 10-, and 5-mol % solutions. The dashed line in (a) is the result for pure water taken from Ref. 62.

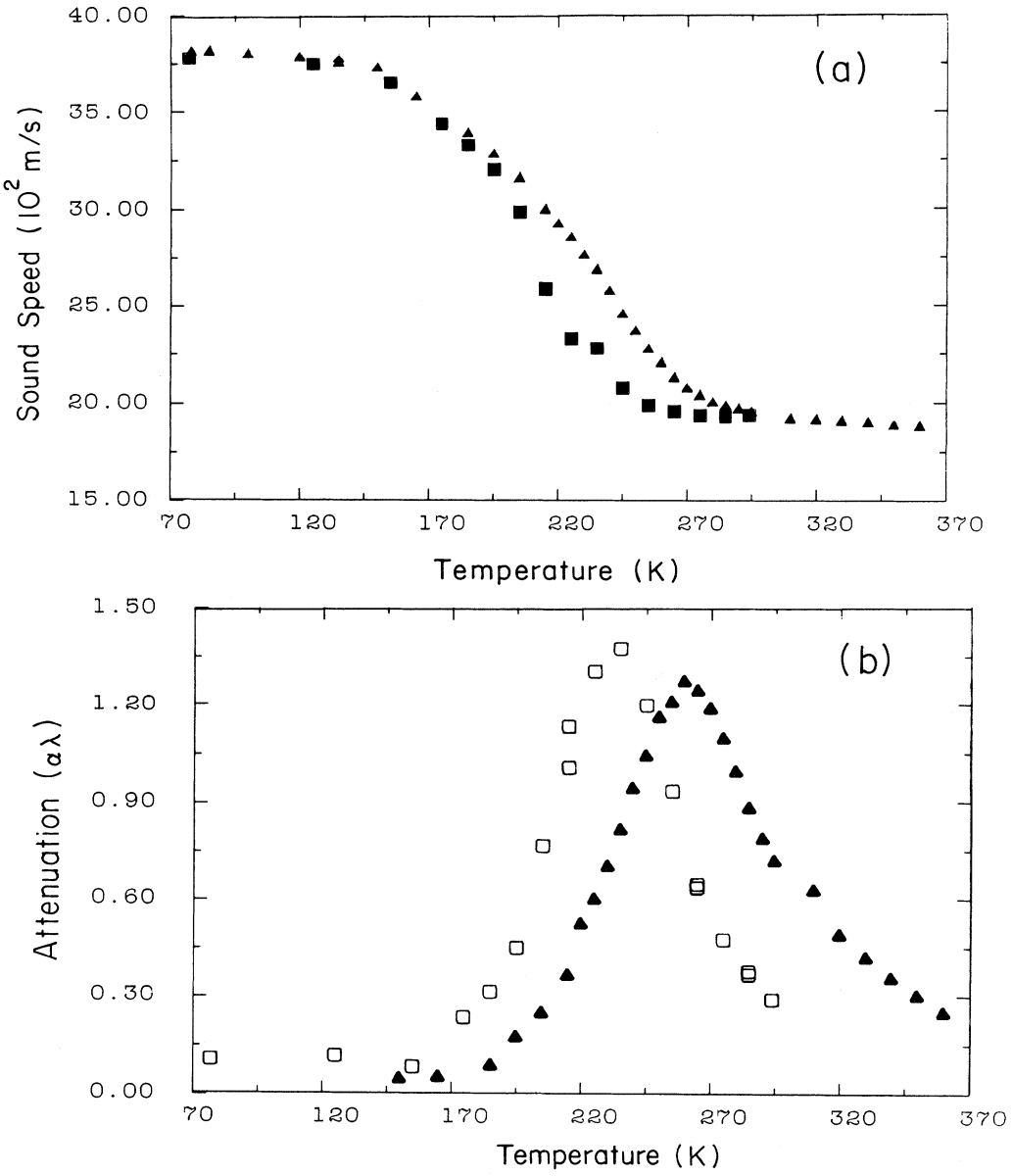

FIG. 5. Comparisons of the speed (a) and attenuation (b) between 90° (▲) and 24.5° (■ or □) scattering for the 15-mol % solution.

V. ANALYSIS OF POLARIZED BRILLOUIN SPECTRA

A. Generalized hydrodynamics

We first analyzed our (VV) Brillouin data by fitting the 1024-point digital spectra to the generalized hydrodynamic result in the long-wavelength limit of Eq. (2.9). In performing the analysis, it is convenient to use the equivalent expression

$$I(\omega)=\frac{I_0}{\omega}\mathrm{Im}\left[\omega_\infty^2-\omega^2-i\omega\gamma_0-\Delta^2\frac{1}{1-i\omega\tau}\right]^{-1}$$
$$=\frac{I_0[\gamma_0+\Delta^2\tau/(1+\omega^2\tau^2)]}{[\omega^2-\omega_0^2-\Delta^2\omega^2\tau^2/(1+\omega^2\tau^2)]^2+\{\omega[\gamma_0+\Delta^2\tau/(1+\omega^2\tau^2)]\}^2}\ , \tag{5.1}$$

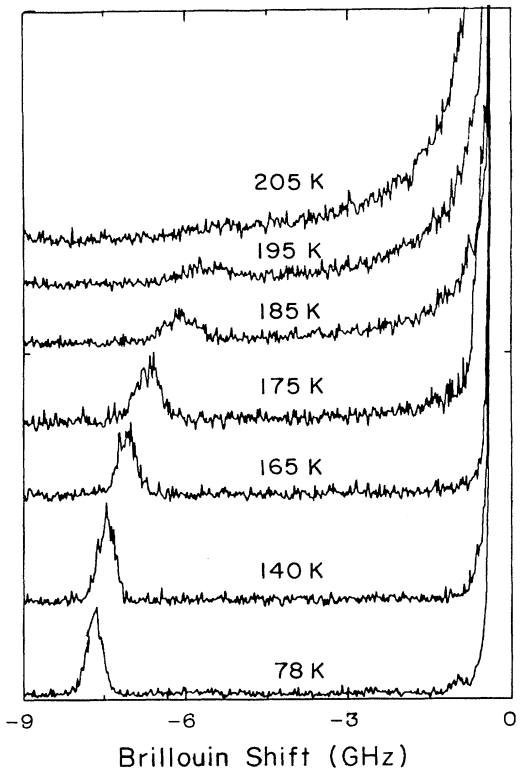

FIG. 6. VH spectrum of the 30-mol% LiCl solution at $\theta=90°$ at 205, 195, 185, 175, 165, 140, and 78 K.

where $\omega_0=C_0k$ is the angular frequency of the Brillouin peak in the low-frequency limit ($\omega_0 t \ll 1$), $\gamma_0=\Phi_0 k^2$ is the background Brillouin linewidth in the high-frequency limit ($\omega_0\tau \gg 1$), and $\Delta^2=\Phi_I k^2$ is the strength of the relaxing part of the longitudinal viscosity. Note that, if $\omega_0\tau \gg 1$, the Brillouin peak shifts from $\omega_0=C_0k$ to

$$\omega_\infty=(\omega_0^2+\Delta^2)^{1/2}=C_\infty k \ ,$$

while if $\omega_0\tau \ll 1$, the Brillouin linewidth increases from γ_0 to $\gamma_0+\Delta^2\tau$. In general, the angular frequency of the Brillouin peak is $\omega_0 \leq \omega_B \leq \omega_\infty$.

Since the spectra at temperatures below 200 K (where $\omega_0\tau \gg 1$) show no relaxation effects, we analyzed the 135-K data as simple Lorentzians to find low-temperature limiting values of ω_∞ and γ_0. The resulting value of $\gamma_0=1.9\times10^9$ rad/s was assumed to be temperature independent. In each fit, k was computed using our room-temperature measurements of the refractive index combined with

$$(dn/dT)=-1.36\times10^{-4}/\mathrm{K}$$

reported by Hsich *et al.*[59]

Spectra were fitted to Eq. (5.1) on the Science Division Vax 11/780 using the Port Library NLLSQ nonlinear least-squares fitting routine. The instrumental response was included by convoluting the computed theoretical spectrum with the strong elastic peak. In each fit, ω_0, Δ, and τ were treated as free fitting parameters along with the normalization constant I_0 and an arbitrary flat background. These five-parameter fits generally resulted in χ^2 valus of less than 2. The results of the fitting procedure for the 15% solutions at $\theta=90°$ are shown by the solid lines in Fig. 3.

We similarly analyzed $\theta=90°$ data for a 30% solution at $T=250$ K. The resulting values of ω_0, Δ, and τ were then used to compute a theoretical spectrum for $\theta=24.5°$. The results, shown in Fig. 8, along with the experimental data indicate that the model works extremely well.

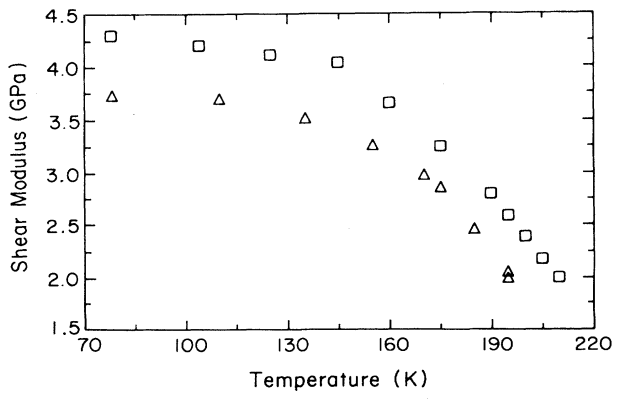

FIG. 7. The shear modulus of the TA mode of 15- (△) and 30- (□) mol % LiCl solutions vs temperature.

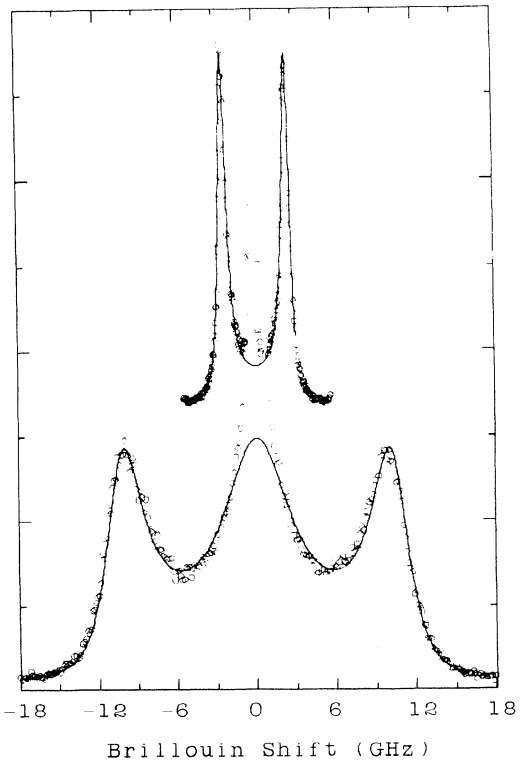

FIG. 8. Brillouin spectra of the 30% solution at $\theta=24.5°$ (top) and 90° (bottom) at $T=250$ K. The circles are the experimental spectra and the solid lines are the calculated spectra. (Only $\frac{1}{3}$ of the data points are shown for clarity.)

The numerical results of the fits for the 15% solution shown in Fig. 3 are tabulated in Table II, along with the longitudinal sound speeds C_0 and C_∞ deduced from the fits. Note that the resulting background kinematic longitudinal viscosity $\Phi_0=3\times10^{-2}$ S is close to the ordinary kinematic viscosity of slightly supercooled water, while the relaxing component $\Phi_l\tau_l$, which is comparable to Φ_0 at 285 K, increased nearly 2 orders of magnitude when T was decreased to 200 K.

We calculated C_0 and C_∞ for all the samples studied from the fitted ω_0 and Δ values, and plotted them as functions of temperature in Fig. 9. Above T_g, the liquid-glass transition temperature determined from heat-capacity measurements,[44,45] C_∞ is a linear function of temperature with a negative slope at each concentration. Below about 200 K, the position of the Brillouin peak is virtually the same as $C_\infty k$, which means that the relaxation time becomes too long to influence the acoustic mode at GHz frequencies. As shown in Fig. 4(a), the speed of the high-frequency LA mode C_∞ has an anomalous change of slope at T_g. This behavior is not understandable in terms of the relaxation model, and we leave the discussion of the origin of this change to Sec. VII. C_0 is also essentially a linear function of temperature for each concentration, but with a positive slope.

So far we have considered only the single-relaxation-time approximation in discussing our data. This approximation can be generalized either by replacing $(1-i\omega\tau)^{-1}$ in Eq. (5.1) by an empirical function such as the Cole-Davidson function $(1-i\omega\tau)^{-\beta}$, or by replacing the ex-

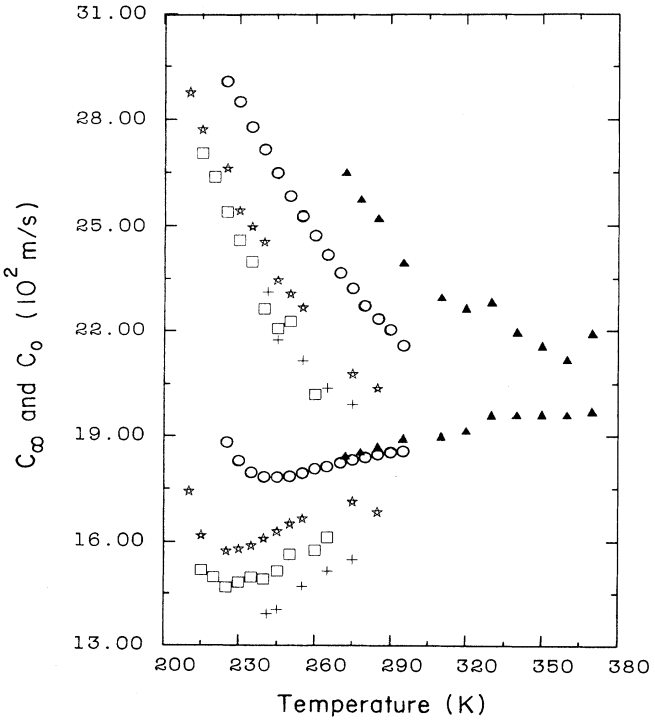

FIG. 9. Fitted high-frequency (C_∞) and low-frequency (C_0) longitudinal sound speeds vs temperature. △, ○, ☆, □, and + corresponds to 36, 30, 15, 10, and 5 mol %, respectively.

TABLE II. Fits of VV Brillouin spectra of 15% LiCl solutions to the generalized hydrodynamic Eq. (2.9).

T (K)	$\omega_0=C_0k$ (10^9 rad/s)	$\gamma_0=\Phi_0k^2$ (10^9 rad/s)	$\Delta^2=\Phi_lk^2$ (10^9 rad/s)^2	τ (sec)	$\omega_\infty=(\omega_0^2+\Delta^2)^{1/2}$ (10^9 rad/s)	k (10^5 cm^{-1})	C_0 (10^5 cm/s)	C_∞ (10^5 cm/s)	Φ_0 (cm^2/s)	$\Phi_l\tau_l$ (cm^2/s)	χ^2
285	42.89	1.9	$(29.24)^2$	5.05×10^{-12}	51.91	2.534	1.693	2.049	3.02×10^{-2}	6.72×10^{-2}	2.7
275	43.66	1.9	$(30.07)^2$	8.29×10^{-12}	53.01	2.536	1.772	2.090	3.02×10^{-2}	1.166×10^{-1}	1.9
255	42.50	1.9	$(39.31)^2$	1.15×10^{-11}	57.89	2.541	1.673	2.278	3.01×10^{-2}	2.75×10^{-1}	1.9
250	42.19	1.9	$(41.11)^2$	1.30×10^{-11}	58.91	2.543	1.659	2.317	3.00×10^{-2}	3.40×10^{-1}	1.9
245	41.64	1.9	$(43.11)^2$	1.48×10^{-11}	59.94	2.544	1.637	2.356	3.00×10^{-2}	4.25×10^{-1}	1.7
240	41.17	1.9	$(47.35)^2$	1.77×10^{-11}	62.75	2.545	1.618	2.466	3.00×10^{-2}	6.13×10^{-1}	1.7
235	40.67	1.9	$(49.29)^2$	2.05×10^{-11}	63.90	2.546	1.597	2.510	3.00×10^{-2}	7.68×10^{-1}	2.0
230	40.47	1.9	$(50.99)^2$	2.27×10^{-11}	65.10	2.548	1.588	2.555	2.99×10^{-2}	9.09×10^{-1}	1.9
225	40.33	1.9	$(54.98)^2$	2.96×10^{-11}	68.19	2.549	1.582	2.675	2.99×10^{-2}	1.38	2.0
215	41.50	1.9	$(57.64)^2$	3.60×10^{-11}	71.03	2.551	1.627	2.784	2.98×10^{-2}	1.84	2.0
210	44.72	1.9	$(58.73)^2$	4.69×10^{-11}	73.82	2.552	1.752	2.893	2.98×10^{-2}	2.48	1.9
200	53.73	1.9	$(55.84)^2$	6.13×10^{-11}	77.49	2.555	2.103	3.033	2.98×10^{-2}	2.93	2.1
135		1.9			91.0	2.571		3.539	2.94×10^{-2}		

ponential form for the viscosity memory function $\Phi_l(t) \propto e^{-t/\tau}$ by the Kohlrausch-Williams-Watts (KKW) or stretched exponential) form $e^{-(t/\tau)^{\beta}}$. (The connection between these two generalizations and their applications to the glass transition in glycerol has been discussed recently by Ngai and Rendell.[65])

We tried fitting our data to Eq. (5.1) with the Cole-Davidson distribution. However, we obtained little improvement when the extra parameter β was used, and we found a strong correlation between β and the coupling constant Δ. The strong correlation cannot be removed even if spectra at different scattering angles are fitted simultaneously. Therefore, it is difficult to determine from Brillouin data alone whether the relaxation process has a distribution of relaxation times or not. One reason for this difficulty is the following. In principle, to tell if the relaxation mode has a single relaxation time, the most straightforward approach is to see if the central mode spectrum has a Lorentzian form when it is decoupled from the LA mode ($\omega_B \gg 1/\tau$) which can be carried out with correlation spectroscopy. Unfortunately, in Brillouin-scattering experiments, the relatively intense Rayleigh scattering blocks a significant part of the central mode when this condition is fulfilled. Therefore, the relaxation times found from our data analysis should be regarded as average relaxation times.

The temperature-dependent relaxation times found from our data analysis for different LiCl concentrations are plotted logarithmically against the inverse temperature in Fig. 10. The plots are essentially linear, indicating that $\tau(T)$ obeys the Arrhenius relation approximately. However, for some concentrations, especially 30 and 36% for which more data points were taken at lower temperatures, we do begin to see a departure from the Arrhenius behavior. This is not surprising if one considers that, according to Angell's classification, the LiCl solution is a fragile liquid,[66] and conductivity relaxation[43,56] and viscosity data[64] show clear non-Arrhenius behavior at low temperatures. Such behavior is usually described by the Vogel-Tammann-Fulcher equation

$$\tau = \tau_0 \exp\left[\frac{B}{T - T_0}\right].$$

Attempts to fit our data to this equation were unsuccssful because the quality of the data was not sufficiently good; the values found for the three parameters τ_0, T_0, and B were highly correlated and gave equally good fits over unacceptably wide ranges. We therefore limited our analysis to the simple Arrhenius relaxation ($T_0 = 0$).

We extracted the activation energy from the slopes of the straight lines in Fig. 10 and listed them in Table III. The activation energy increases from 2 Kcal/mol at 36 mol% to 6 Kcal/mol at 5 mol%. We note that the energy for breaking a hydrogen bond is about 2 Kcal/mol;[67]

TABLE III. Activation energies (E) vs concentration (C) from the Arrhenius plots of Fig. 10.

C (mol%)	5	10	12	15	30	36
E (kcal/m)	5.8	4.2	4.3	3.3	2.5	2.3

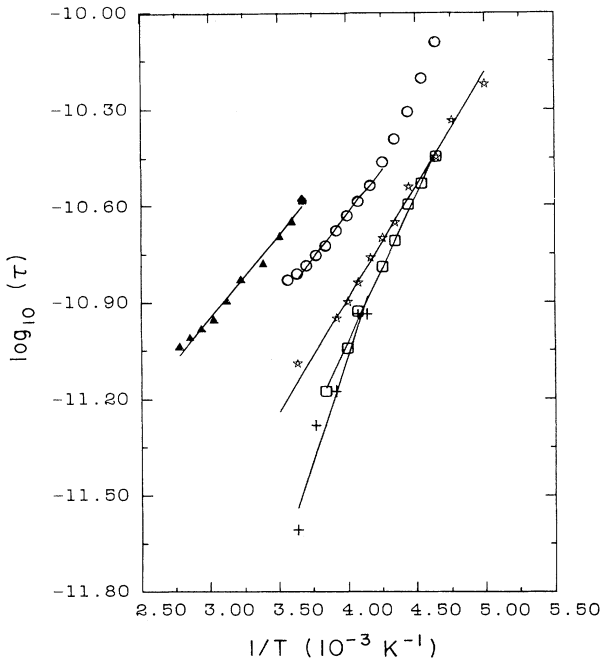

FIG. 10. Arrhenius plots of $\log_{10}\tau$ vs $(1/T)$ for 36- (▲), 30- (○), 15- (☆), 10- (□), and 5- (+) mol% LiCl solutions. The solid lines are fitted results using the Arrhenius relation.

therefore, our results may suggest that the average number of hydrogen bonds increases from about 1 at 36 mol% to 3 at 5 mol%. The value of 6 Kcal/mol at 5 mol% is consistent with 7 Kcal/mol for pure water found from the dielectric-constant measurements, but is in sharp contrast to the value of 20 Kcal/mol estimated in Ref. 62 from Brillouin scattering in supercooled water. At room temperature, the relaxation is slower for higher-concentration samples.

B. Mode coupling

In Sec. III we showed how an approximate form of the mode-coupling theory can be exploited to predict the spectrum $S(k,\omega)$ in the small-k regime appropriate to Brillouin-scattering experiments. The results of that calculation were shown in Fig. 2. We have not attempted a quantitative fit of our data to the mode-coupling predictions, but have compared the experimental and theoretical results for the Brillouin shifts and linewidths.

In Fig. 11 we show the experimentally determined Brillouin shifts for the 15% solution at $\theta = 90°$ by the small triangles. The predictions of the mode-coupling calculations, with no adjustment, are shown by the ☆ symbols. Since this result produces negligible temperature dependence, we arbitrarily increased the coupling strength λ in Eq. (3.6) by a factor of 7 to obtain a result qualitatively similar to the experimental values as shown by the squares in Fig. 11(a). The corresponding Brillouin

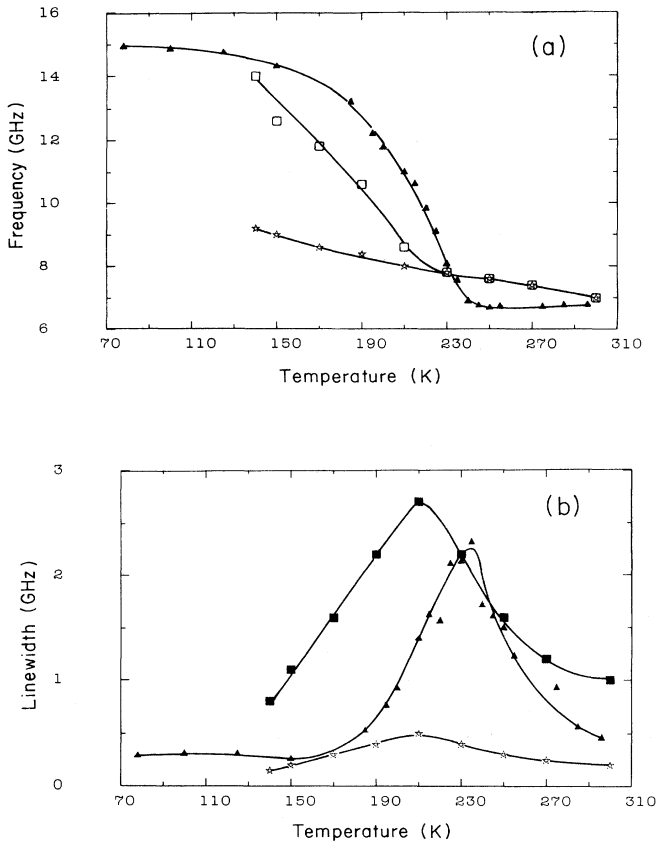

FIG. 11. The mode-coupling predicton for the Brillouin shift (a) and Brillouin linewidth (b) with no adjustment (☆) and with the coupling constant λ multiplied by 7 (□ or ■) compared with the experimental results (▲).

linewidths are shown in Fig. 11(b). Again, the mode-coupling theory without adjustment produces clearly insufficient broadening. Increasing λ by a factor of 7 results in predictions which are qualitatively similar to the experimental values, but quantitatively are clearly different. In particular, note that the predicted linewidth decreases rather slowly as the glass transition is approached, while the experimental linewidth decreases very rapidly. We will discuss this difference further in Sec. VII.

VI. DEPOLARIZED SCATTERING

The transverse part of the linearized Navier-Stokes equation for a simple fluid is solved by a transverse velocity correlation function [Boon and Yip,[36] Eq. (6.2.5)]

$$J_T(k,\omega)=2v_0^2\frac{\nu k^2}{\omega^2+(\nu k^2)^2}\ , \tag{6.1}$$

where $\nu=\eta_s/\rho_0$ is the kinematic shear viscosity.

The two orthogonal nonpropagating transverse hydrodynamic modes (viscous shear modes) described by Eq. (6.1) are decoupled from the other degrees of freedom and the refractive index unless a temperature gradient is present,[68] and therefore do not scatter light. If the liquid consists of optically anisotropic molecules, however, orientational fluctuations will couple to the transverse shear modes and can produce a depolarized quasielastic spectrum with a dip at $\omega=0$ due to interference effects. This effect was investigated experimentally, e.g., by Stegeman, Stoicheff and Enright;[69] the theory has been reviewed by Berne and Pecora.[70]

In solids, transverse displacements associated with propagating transverse acoustic modes can scatter light even in isotropic materials, since the photoelastic (Pockels) effect allows coupling of shear strain to the refractive index in all crystal classes.[71] Light scattering from fully resolved transverse acoustic modes in silica glass, for example, can be easily observed in Brillouin scattering.[72]

Well-resolved transverse modes, such as those shown in Fig. 6, have been observed in the depolarized Brillouin spectra of numerous undercooled liquids, near the glass transition, including salol,[12,13] triphenylphosphite,[17] $ZnCl_2$,[20] B_2O_3,[18,19] and [60% KNO_3–40% $Ca(NO_3)_2$].[19,22,23] In most cases, the transverse acoustic modes which are sharp near T_g, broaden and move gradually towards lower frequency as T increases, and are eventually "engulfed" by the central component. Since we are interested in the oscillatory transverse shear modes at low temperatures and not in the detailed form of the spectrum near $\omega=0$, we will not consider the role of molecular anisotropy, but will rather utilize a simple version of the viscoelastic theory proposed by Rytov.[69,73,74] Wang and Zhang[13] have analyzed VH polarized Brillouin spectra of salol using a version of the Rytov theory in which optical coupling occurs through the anisotropic polarizability of the molecules, and also included viscoelastic behavior in the shear viscosity. We do not distinguish between optical coupling via molecular reorientation or via local structural deformation, but simply assume that the off-diagonal components of the dielectric tensor couple to the local shear strain via a frequency-dependent Pockel's coefficient $p(\omega)$ which (as assumed by Rytov) has the same relaxation time as the shear viscosity. By analogy with the dynamic structure factor $S(k,\omega)$, we define the shear strain correlation function

$$S_T=\left[\frac{k}{\omega}\right]^2 J_T(k,\omega)\ ,$$

so that the depolarized scattered spectrum $I_{\rm VH}(\omega)$ is given by

$$I_{\rm VH}(\omega)\simeq\frac{I_0 p(\omega)}{\omega^2}J_T(k,\omega)\ . \tag{6.2}$$

As shown by Boon and Yip, the transverse current correlation function [Eq. (6.1)] can be generalized for relaxing fluids by replacing ν by a memory function $K_T(t)$. The value of this function at time $t=0$ is $K_T(t=0)=\mu_\infty/\rho$, where μ_∞ is the high-frequency shear modulus, while $\lim_{\omega\to 0}K_T'(\omega)=\nu$, the kinematic shear viscosity. In the single-exponential approximation

$$K_T(t)=K_0\exp(-t/\tau_T)$$

(Maxwell viscoelasticity), Eq. (6.2) for $I_{\rm VH}(\omega)$ becomes

$$I_{\mathrm{VH}}(\omega)=\frac{I_0 p(\omega)K_0\tau_T/(1+\omega^2\tau_T^2)}{[\omega^2-k^2K_0\omega^2\tau_T^2/(1+\omega^2\tau_T^2)]^2+[\omega k^2K_0\tau_T/(1+\omega^2\tau_T^2)]^2}\ . \tag{6.3}$$

Note that Eq. (6.3) is similar to Eq. (2.9), except that the $C_0^2k^2=\omega_0^2$ term is missing, and τ_T is the transverse (as opposed to longitudinal) relaxation time. As shown by Boon and Yip, Eq. (6.3) will exhibit propagating modes if $k^2K_0>1/(2\tau_T^2)$. As $\tau_T\to\infty$, Eq. (6.3) predicts sharp Brillouin components at $\omega_T=\pm k(K_0)^{1/2}$, in agreement with the usual result for solids

$$\omega_T=\pm k(\mu_\infty/\rho_0)^{1/2}\ .$$

We evaluated Eq. (6.3) using a relaxing photoelastic constant

$$p(\omega)=(\omega\tau_T)^2/[1+(\omega\tau_T)^2]$$

and setting $k^2K_0=(50\times10^9)^2$ which fixes the low-T Brillouin peaks at $\sim$8 GHz. (Propagating modes are then expected for $\tau_T>10^{-11}$ s.) τ_T was then varied from 1.0×10^{-9} to 5×10^{-12} s producing the series of theoretical spectra shown in Fig. 12. These spectra are qualitatively similar to the experimental results, except that the position of the Brillouin peak changes very little with temperature. In order to match the experimental results, the intrinsic temperature dependence of K_0 should also be included. Given the low signal-to-noise ratio of our data, we have not attempted a quantitative fit. However, the crossover from propagating to nonpropagating behavior at $\sim$200 K implies that, at 200 K, $\tau_T\sim1\times10^{-11}$ s, while extrapolating from Fig. 10, we find that, at 200 K, the longitudinal relaxation time for the 30% solution is $\sim2\times10^{-10}$ s.

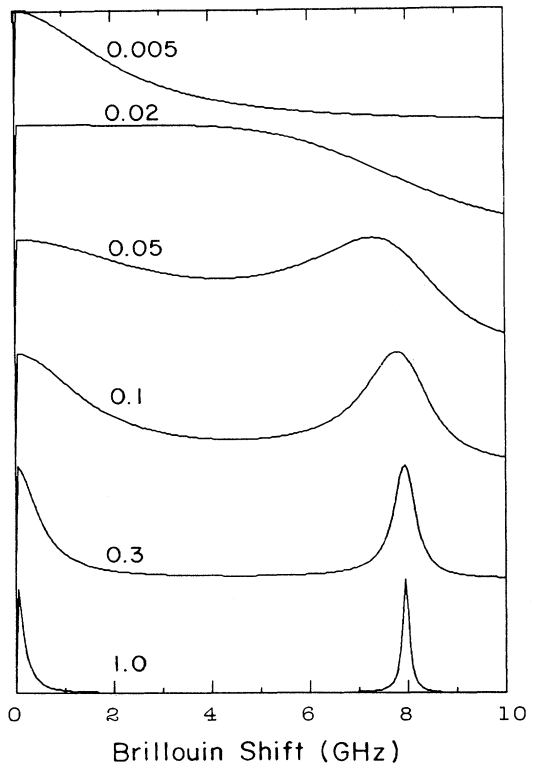

FIG. 12. Theoretical VH Brillouin spectra predicted by Eq. (6.3) for values of τ_T between 0.005 and 1.0×10^{-9} s.

VII. DISCUSSION AND CONCLUSIONS

A. Generalized hydrodynamics

We have shown that the VV-polarized Brillouin spectra can be accurately fit by the dynamic structure factor $S(K,\omega)$ predicted by generalized hydrodynamics, classical viscoelasticity, or the Mountain theory (all being equivalent in the long-wavelength intermediate-frequency regime studied in Brillouin scattering). The concentration- and temperature-dependent longitudinal relaxation time $\tau_l(T)$ found from single-exponential-relaxation analysis obeys the Arrhenius law over a wide range of temperatures and concentrations. VH spectra, although of insufficient quality for an equivalent quantitative analysis, also agreed with the predictions of viscoelastic theory qualitatively, although the transverse-relaxation time τ_T appears to be somewhat shorter than τ_l.

Although structural relaxation times have been measured in many systems by Brillouin and ultrasonic experiments, their microscopic origins are generally not clear. To get some insight into the mechanism of the structural relaxation found from our Brillouin data, we also compared the results for τ_l with the relaxation times measured by other techniques in similar frequency and temperature ranges.

The reorientational relaxation time of water molecules in LiCl solutions has been determined from depolarized light-scattering spectra.[58] Though at room temperature the relaxation time is of the same order of magnitude as the structural relaxation time, and both follow the Arrhenius relation in the measured temperature ranges, the activation energies are about twice as large for reorientation as for structural relaxation. So we rule out the possibility that the structural relaxation is simply due to the reorientation of the water molecules in the solution.

B. Mode-coupling theory

Our mode-coupling analysis has shown that the qualitative aspects of the changes in the Brillouin spectrum can be explained by this theory, but the quantitative predictions of the mode-coupling theory are disappointing. First, the predicted dispersion and broadening effects are too small, unless the coupling constant is arbitrarily increased by about seven times. Second, the excess broadening near $\omega\tau=1$ decreases much more dramatically as T is further decreased in the experimental data than in the theoretical predictions. We attribute this second

problem to the fact that, in the mode-coupling theory, even though the slow-relaxation process narrows to a δ function at T_g, there is still a large fast-relaxation process with 50% of the total damping strength, which continues to produce excess broadening of the Brillouin peaks even below T_g. Neutron spin-echo studies of [60% KNO_3–40% $Ca(NO_3)_2$] (Ref. 25) and polybutadiene[26,27] indicate that the slow-relaxing component accounts for $\sim$90% of the relaxation near T_g rather than 50%. Of course, our calculation employed a very simplified version of the mode-coupling theory in which only modes with $|k|=k_0$ were included in the integrals. However, Bengtzelius *et al.*[9] showed that this approximation has negligible effect on the coupling strength, and Kirkpatrick[40] has shown that, in the calculation of η_s and D, inclusion of the full range of k values leads to only minor changes of $\sim$10%. Other possible sources of disagreement are the use of the hard-sphere model, or that only the leading two-mode term in the theory has been included, while higher-order processes may become important near T_g.

C. Nature of the glass transition

Our Brillouin-scattering results show that the temperature-dependent sound speeds of the LA mode [Fig. 4(b)] and TA mode (Fig. 7) both exhibit a discontinuous change of slope at T_g, where $T_g=145$ K for the 15% solution is the transition temperature determined by Angell *et al.* from heat-capacity measurements.[45] Since our average cooling rate was $\sim$1 K/min, which is close to the cooling rate used in the heat-capacity measurements, the same value of T_g should apply. We note that similar slope changes were observed in Brillouin-scattering studies of $ZnCl_2$,[21] [60%KNO_3–40% $Ca(NO_3)_2$] (Refs. 19 and 23) and B_2O_3,[18] but this result has not been discussed previously.

Such behavior is clearly not expected within the framework of any kinetic theory of the glass transition since the $\omega\tau=1$ crossover for the high-frequency Brillouin modes occurs far above T_g. We note that, in the version of the mode-coupling theory by Leutheuser,[8] the LA and TA sound speeds near T_g are given by $(1+4\lambda f^2)^{1/2}$ and $(\lambda f^2)^{1/2}$, respectively, where $f=\frac{1}{2}(1+\sqrt{1-1/\lambda})$ and λ is the coupling constant [see Eq. (3.7)], which is related to the static structure factor, and is expected to increase as temperature decreases. Thus, the speeds of both LA and TA modes are expected to increase as temperature decreases in the liquid phase, as observed. Below T_g, where λ is a weak function of temperature, the sound speeds would be relatively constant. However, this theory agrees with computer simulations only for $\eta_s \leq 100$ poise,[9] and therefore may not be applicable to the region around T_g.

The slope change seen in the sound speeds at T_g might be a result of a structure change at T_g signaling a true thermodynamic phase transition to a glassy state fundamentally distinct from the undercooled liquid above T_g. In fact, Wendt and Abraham[13] found a change for the ratio of the maximum and minimum of $S(\mathbf{k})$ at the glass transition. A possible explanation is provided by the rigidity percolation theory. For network glasses, a large increase in the elastic constants as a result of increasing the bond coordination number at a percolation threshold was predicted by He and Thorpe[75] and confirmed experimentally by Halfpap and Lindsay.[76] A free-volume model combined with the idea of percolation, developed by Cohen and Grest,[7] describes the change of viscosity as well as the thermodynamic quantities, specific heat, and thermal expansion successfully. According to this theory, a glass-forming system consists of solidlike and liquidlike cells. As the temperature increases, the fraction of liquidlike cells p increases. When p is larger than a percolation threshold p_c there is an infinite, connected, liquidlike cluster and the material is in the liquid state; when p is less than p_c, it is in the glass state. Using this picture, one might expect that the contribution to the speed of sound waves from the solidlike clusters would be larger than that of liquidlike clusters, and would decrease as p increases.

ACKNOWLEDGMENTS

We wish to thank C. A. Angell, M. H. Cohen, and R. D. Mountain for helpful discussions. This research was supported initially by National Science Foundation (NSF) Grant No. DMR-8614168 and subsequently by the Science Division and Physics Department of City College of New York (CCNY).

[1]G. H. Fredrickson, Annu. Rev. Phys. Chem. **39**, 149 (1988).
[2]J. Jackle, Rep. Prog. Phys. **49**, 171 (1986).
[3]J. Wong and C. A. Angell, *Glass* (Marcel Dekker, New York, 1976).
[4]K. L. Ngai, R. W. Rendell, A. K. Rajagopal, and S. Teitler, in *Dynamic Aspects of Structure Change in Liquids and Glasses, New York, 1985,* edited by C. A. Angell and M. Goldstein [Ann. N.Y. Acad. Sci. **484**, 150 (1986)].
[5]*The Glass Transition and the Nature of the Glassy State, New York, 1975,* edited by M. Goldstein and R. Simha [Ann. N.Y. Acad. Sci. **279**, (1976)].
[6]*Structure and Mobility in Molecular and Atomic Glasses, New York, 1980,* edited by J. M. O'Reilly and M. Goldstein [Ann. N.Y. Acad. Sci. **371**, (1981)].
[7]M. H. Cohen and G. S. Grest, Phys. Rev. B **20**, 1077 (1979).
[8]E. Leutheusser, Phys. Rev. A **29**, 2765 (1984).
[9]U. Bengtzelius, W. Gotze, and A. Sjolander, J. Phys. C **17**, 5915 (1984).
[10]C. A. Angell and L. M. Torell, J. Chem. Phys. **78**, 937 (1983).
[11]L. V. Woodcock and C. A. Angell, Phys. Rev. Lett. **47**, 1129 (1981).
[12]G. D. Enright and B. P. Stoicheff, J. Chem. Phys. **64**, 3658 (1976).
[13]C. H. Wang and J. Zhang, J. Chem. Phys. **85**, 794 (1986).
[14]Y. Y. Huang, E. A. Friedman, R. D. Andrews, and T. R. Hart, in *Light Scattering in Solids,* edited by M. Balkanski

(Flammarion, Paris, 1971), p. 488.
[15]E. A. Friedman and A. J. Ritger, J. Appl. Phys. **40**, 4243 (1969).
[16]P. Bezot, C. Hesse-Bezot, J. P. Petitet, and D. Roynard, J. Mol. Liq. **34**, 317 (1987).
[17]D. G. Miles, Jr., N. Le, and D. Kivelson, J. Chem. Phys. **90**, 5327 (1989).
[18]T. Yagi, Physica B **150**, 265 (1988).
[19]M. Grimdsditch, R. Bhadra, and L. M. Torell, Phys. Rev. Lett. **62**, 2616 (1989).
[20]H. E. Gunilla Knape, J. Chem. Phys. **80**, 4788 (1984).
[21]M. Soltswisch, J. Sukmanowski, and D. Quitmann, J. Chem. Phys. **86**, 3207 (1986).
[22]L. M. Torell, J. Chem. Phys. **76**, 3467 (1982).
[23]L. M. Torell and R. Aronsson, J. Chem. Phys. **78**, 1121 (1983).
[24]P. Taborek, R. N. Kleiman, and D. J. Bishop, Phys. Rev. B **34**, 1835 (1986).
[25]F. Mezei, W. Knaak, and B. Farago, Phys. Rev. Lett. **58**, 571 (1987).
[26]D. Richter, B. Frick, and B. Farago, Phys. Rev. Lett. **61**, 2465 (1988).
[27]B. Frick, B. Farago, and D. Richter, Phys. Rev. Lett. **24**, 2921 (1990).
[28]R. D. Mountain, J. Res. Natl. Bur. Stand. Sect. A **70**, 207 (1966).
[29]R. D. Mountain, Crit. Rev. Solid State Sci. **1**, 5 (1970).
[30]C. J. Montrole, V. A. Slovyev, and T. A. Litovitz, J. Acoust. Soc. Am. **43**, 117 (1968).
[31]R. D. Mountain, J. Res. Natl. Bur. Stand. Sect. A **72**, 95 (1968).
[32]R. Zwanzig, J. Chem. Phys. **43**, 714 (1965).
[33]C. Allain-Demoulin, P. Lallemand, and N. Ostrowsky, Mol. Phys. **31**, 581 (1976); C. Allain-Demoulin, A. M. Cazabat, P. Lallemand, and N. Ostrowsky, Opt. Commun. **15**, 126 (1975).
[34]J. A. Cowen, C. Allain, and P. Lallemand, J. Phys. Lett. (Paris) **37**, L313 (1976); C. Allain and P. Lallemand, J. Phys. (Paris) **40**, 693 (1979); C. Allain, M. Berard, and P. Lallemand, Mol. Phys. **41**, 429 (1980).
[35]D. L. Sidebottom and C. M. Sorensen, Phys. Rev. B **40**, 461 (1989).
[36]J. P. Boon and S. Yip, *Molecular Hydrodynamics* (McGraw-Hill, New York, 1980).
[37]U. Bengtzelius and L. Sjorgen, J. Chem. Phys. **84**, 1744 (1986).
[38]U. Bengtzelius, Phys. Rev. A **34**, 5059 (1986).
[39]W. Gotze and L. Sjorgen, J. Phys. C **20**, 879 (1987).
[40]T. R. Kirkpatrick, Phys. Rev. A **31**, 939 (1985).
[41]M. C. Marchetti, Phys. Rev. A **33**, 3363 (1986).
[42]N. W. Ashcroft and J. Lekner, Phys. Rev. **145**, 83 (1966).
[43]C. T. Moynihan, R. D. Bressel, and C. A. Angell, J. Chem. Phys. **55**, 4414 (1971).
[44]C. A. Angell and E. J. Sare, J. Chem. Phys. **49**, 4713 (1968).
[45]C. A. Angell, E. J. Sare, J. Donella, and D. R. MacFarlane, J. Phys. Chem. **85**, 1481 (1981).
[46]J. Dupuy, J. F. Jal, C. Ferradou, P. Chieux, A. F. Wright, R. Calemczuk, and C. A. Angell, Nature **296**, 138 (1982).
[47]P. Carmona, A. Aouizerat-Elarby, J. F. Jal, J. Dupuy, B. Croset, and P. Chieux, Phase Transitions **14**, 11 (1989).
[48]A. Elarby-Aouizerat, J. F. Jal, P. Chieux, J. M. Letoffe, P. Claudy, and J. Dupuy, J. Non-Cryst. Solids **104**, 203 (1988); A. Elarby-Aouizerat, J. Dupuy, J. M. Letoffe, P. Claudy, and P. Chieux, Ann. NY Acad. Sci. **484**, 302 (1986).
[49]D. M. Soumpasis, J. Wiechen, and T. M. Jovin, J. Biomol. Struct. Dyn. **4**, 535 (1987).
[50]T. Weidlich, S. M. Lindsay, and A. Rupprecht, Phys. Rev. Lett. **61**, 1674 (1988).
[51]J. E. Enderby and G. W. Neilson, Rep. Prog. Phys. **44**, 594 (1981).
[52]M. Magini, in *Ions and Molecules in Solution,* edited by N. Tanaka, H. Ohtaki, and R. Tamamushi (Elsevier, Netherlands, 1983).
[53]J. E. Enderby and G. W. Neilson, Adv. Phys. **29**, 323 (1980).
[54]N. A. Hewish, J. E. Enderby, and W. S. Howells, Phys. Rev. Lett. **48**, 756 (1982).
[55]R. Pottel, in *Water: A Comprehensive Treatise,* edited by F. Frank (Plenum, New York, 1973), Vol. 3.
[56]S. Sridhar and P. Taborek, J. Chem. Phys. **88**, 1170 (1988).
[57]H. G. Hertz, in *Water: A Comprehensive Treatise,* edited by F. Frank (Plenum, New York 1973), Vol. 3.
[58]N. J. Tao and S. M. Lindsay, J. Phys.: Condens. Matter **1**, 8709 (1989).
[59]S. Y. Hsich, R. W. Gammon, P. B. Macedo, and C. J. Montrose, J. Chem. Phys. **56**, 1663 (1972).
[60]J. R. Sandercock, in *Proceedings of the VIIth International Conference on Raman Spectroscopy,* edited by W. F. Murphy (North-Holland, Amsterdam, 1980), p. 364.
[61]S. M. Lindsay, W. M. Anderson, and J. R. Sandercock, Rev. Sci. Instrum. **52**, 1478 (1981).
[62]G. Maisano, P. Migliardo, F. Aliotta, C. Vasi, F. Wanderligh, and G. D'Arrigo, Phys. Rev. Lett. **52**, 1025 (1984).
[63]C. A. Angell, Annu. Rev. Phys. Chem. **34**, 593 (1983).
[64]C. T. Moynihan, N. Balitactac, L. Boone, and T. A. Litovitz, J. Chem. Phys. **55**, 3013 (1971).
[65]K. L. Ngai and R. W. Rendel, Phys. Rev. B **41**, 754 (1990).
[66]C. A. Angell, J. Non-Cryst. Solids **73**, 1 (1985).
[67]C. J. Montrose, J. A. Bucaro, J. Marshall-Coakley, and T. A. Litovitz, J. Chem. Phys. **12**, 5025 (1974).
[68]B. M. Law, P. N. Segre, R. W. Gammon, and J. V. Sengers, Phys. Rev. A **41**, 816 (1990).
[69]G. I. A. Stegemen and B. P. Stoicheff, Phys. Rev. Lett. **21**, 202 (1968); G. D. Enright, G. I. A. Stegeman, and B. P. Stoicheff, J. Phys. (Paris) Colloq. **33**, C1-207 (1972).
[70]B. J. Berne and R. Pecora, *Dynamic Light Scattering* (Wiley, New York, 1976).
[71]J. F. Nye, *Physical Properties of Crystals* (Oxford University Press, New York, 1964).
[72]S. M. Shapiro, R. W. Gammon, and H. Z. Cummins, Appl. Phys. Lett. **9**, 157 (1968).
[73]S. M. Rytov, Zh. Eksp. Teor. Fiz. **33**, 514 (1958) [Sov. Phys. JETP **6**, 401 (1958)]; **33**, 69 (1958) [**6**, 513 (1958)].
[74]G. I. A. Stegeman and B. P. Stoicheff, Phys. Rev. A **7**, 1160 (1973).
[75]H. He and M. F. Thorpe, Phys. Rev. Lett. **54**, 2107 (1985).
[76]B. Halfpap and S. M. Lindsay, Phys. Rev. Lett. **57**, 847 (1986).